nature microbiology

LETTERS

https://doi.org/10.1038/s41564-018-0174-y

# Retraction of DNA-bound type IV competence pili initiates DNA uptake during natural transformation in *Vibrio cholerae*

Courtney K. Ellison[1], Triana N. Dalia[1], Alfredo Vidal Ceballos[2,3], Joseph Che-Yen Wang[4], Nicolas Biais[2,3], Yves V. Brun[1] and Ankur B. Dalia[1*]

**Natural transformation is a broadly conserved mechanism of horizontal gene transfer in bacterial species that can shape evolution and foster the spread of antibiotic resistance determinants, promote antigenic variation and lead to the acquisition of novel virulence factors. Surface appendages called competence pili promote DNA uptake during the first step of natural transformation[1]; however, their mechanism of action has remained unclear owing to an absence of methods to visualize these structures in live cells. Here, using the model naturally transformable species *Vibrio cholerae* and a pilus-labelling method, we define the mechanism for type IV competence pilus-mediated DNA uptake during natural transformation. First, we show that type IV competence pili bind to extracellular double-stranded DNA via their tip and demonstrate that this binding is critical for DNA uptake. Next, we show that type IV competence pili are dynamic structures and that pilus retraction brings tip-bound DNA to the cell surface. Finally, we show that pilus retraction is spatiotemporally coupled to DNA internalization and that sterically obstructing pilus retraction prevents DNA uptake. Together, these results indicate that type IV competence pili directly bind to DNA via their tip and mediate DNA internalization through retraction during this conserved mechanism of horizontal gene transfer.**

It is widely believed that competence pili bind to extracellular DNA and then actively translocate this DNA across the outer membrane via retraction[2,3]. In the predominant alternate model, competence pili act as gatekeepers to open the outer membrane secretin pore via their dynamic activity, allowing for passive DNA diffusion across the outer membrane[4]. The main distinction between the proposed models for DNA uptake is the ability of pili to bind to DNA. Previously, pilus–DNA binding was visually assessed by electron microscopy, which provides a static view and makes differentiating between coincidental co-localization and de facto binding difficult[5]. To test these models directly, we sought to observe both pili and DNA by fluorescence microscopy. Type IV competence pili are dynamic surface appendages that are polymerized and extended via the action of an ATPase, PilB, and retracted by depolymerization via the action of an antagonistic ATPase, PilT. We first labelled type IV competence pili in a hyperpiliated *pilT* mutant of *Vibrio cholerae*[6,7], using a technique[8] in which an amino acid residue of the major pilin subunit PilA is replaced by a Cys for subsequent labelling with a thiol-reactive fluorescent maleimide dye (Alexa-Fluor 488 $C_5$ maleimide (AF488-mal)) (Supplementary Fig. 1a–c). Neither the Cys mutation nor labelling with AF488-mal substantially affected the transformation frequency either in wild-type cells or in a constitutively competent strain in which *pilT* is intact (Supplementary Fig. 1d,e). The constitutively competent strain maintained competence for an extended period of time (≥3 hours) (Supplementary Fig. 2). Because we sought to characterize the function of type IV competence pili downstream of competence induction, we used constitutively competent strains throughout the remainder of the study.

To directly observe pilus–DNA binding, we fluorescently labelled both pili and DNA and tracked them by microscopy in real time. Imaging revealed several cells harbouring DNA-bound pili, and adherence was evident from the co-localized movement of DNA and pili (Fig. 1a and Supplementary Video 1). We further confirmed DNA adherence using sheared pili bound to microfluidic channels by observing the correlated movement of DNA with single pilus fibres along with subsequent DNA detachment when flow was maintained (Fig. 1b, Supplementary Fig. 3 and Supplementary Videos 2 and3). We found that the majority of DNA interactions occurred at the pilus tip (Fig. 1c). DNA-binding assays with fluorescently labelled DNA demonstrated that the piliated *pilA*-Cys and parent strains bound DNA equally, whereas the non-piliated *pilA* mutant was deficient in DNA binding (Fig. 1d). Furthermore, competition assays with unlabelled competitors indicated that this binding was specifically inhibited by nucleic acids with a strong preference for double-stranded DNA (dsDNA) (Fig. 1e). This result is consistent with dsDNA binding to *Streptococcus pneumoniae* competence pili[5] and the preferential uptake of dsDNA in *Neisseria* spp.[9], although single-stranded DNA (ssDNA) can be transformed with similar efficiency in the latter[10]. Importantly, we found that DNA binding was dependent on the pilus fibre and could not be attributed to the outer membrane secretin[11,12], which still localized properly in the *pilA* mutant (Supplementary Fig. 4a–c). Thus, type IV competence pili specifically bind to extracellular dsDNA.

Because the majority of DNA binding occurs at the pilus tip, we hypothesized that retraction helps to bring tip-bound DNA to the cell. Indeed, we found that type IV competence pili are highly active surface structures, with 47% of cells grown under competence-inducing conditions making at least one pilus of an average length of ~1.0 μm within a 1-minute period (Fig. 2a,b, Supplementary Fig. 5a–c and Supplementary Video 4). Extension and retraction rates of type IV competence pili were significantly different, with retraction occurring twice as fast (Supplementary Fig. 5b). However, pilus dynamic activity was not altered by the presence of extracellular DNA (Supplementary Fig. 6). In some cases, cells synthesized pili repeatedly at the same site, suggesting that the same assembly

[1]Department of Biology, Indiana University, Bloomington, IN, USA. [2]Biology Department, CUNY Brooklyn College, Brooklyn, NY, USA. [3]Graduate Center of CUNY, New York, NY, USA. [4]Electron Microscopy Center, Indiana University, Bloomington, IN, USA. *e-mail: ankdalia@indiana.edu

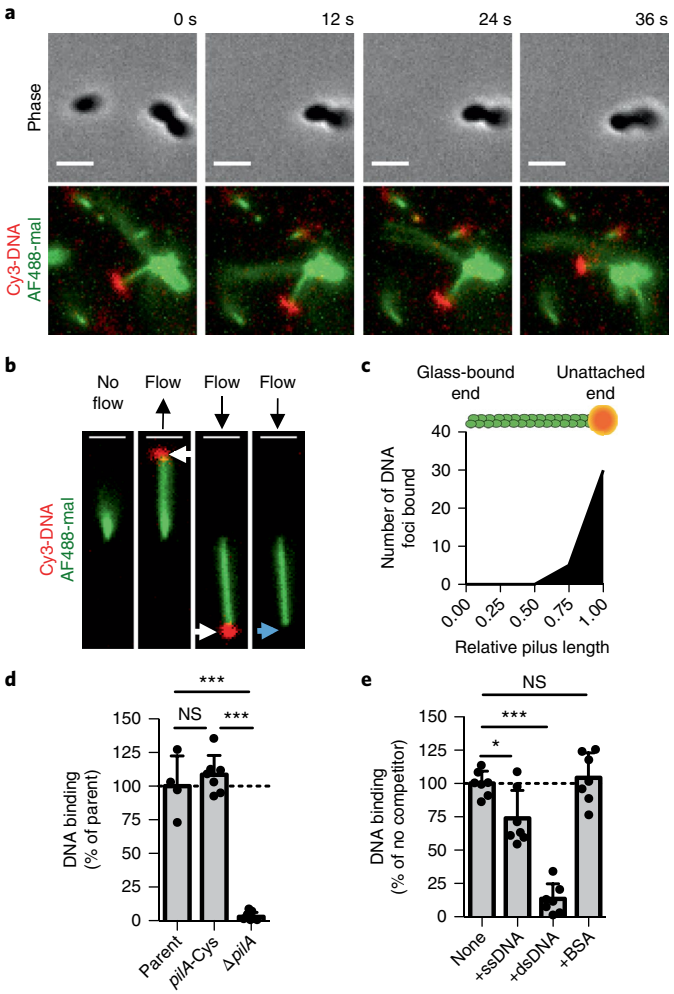


**Fig. 1 | The tips of type IV competence pili directly bind to DNA.** Because type IV competence pili are dynamically active and relatively few pili are extended at any given time, all pilus–DNA binding studies were performed in Δ*pilT* backgrounds to ensure that cells contained numerous extended pili, as shown in Supplementary Fig. 1c. **a**, A montage of time-lapse imaging of a *pilA*-Cys Δ*pilT* cell labelled with AF488-mal after mixing with Cy3-labelled DNA in a wet mount. Scale bars, 2 µm. **b**, An example of a sheared pilus labelled with AF488-mal bound to glass within a microfluidic device after the addition of fluorescently labelled DNA. Before flow is applied, the relatively long pilus fibre is out of the field of view, but after flow is applied, bound DNA becomes apparent (white arrows) and moves with the direction of flow. When flow is maintained, the DNA detaches from the pilus fibre (blue arrow). Black arrows above the images represent the direction of flow. Scale bars, 2 µm. Data in panels **a** and **b** are representative of three independent experiments. **c**, Localization of bound DNA along sheared pili in microfluidic devices. Pili were normalized in length to 1.00 (arbitrary units), and the position of DNA foci bound along the length for each fibre was plotted; $n = 51$ independent DNA-bound pili analysed. The green rod above the plot is a visual representation of a labelled pilus fibre bound to orange DNA. **d**, The relative DNA-binding assay using a fluorescently labelled 6-kb PCR product. Parent: $n = 4$, *pilA*-Cys: $n = 7$ and Δ*pilA*: $n = 7$. **e**, The relative DNA binding as in panel **d** except with the addition of the indicated non-labelled competitors at 50-fold excess. Competitors were ssDNA (PhiX174 virion), dsDNA (PhiX174 RFII) or bovine serum albumin (BSA). $n = 7$ for all samples. Each data point in panels **d** and **e** represents an independent biological replicate, and the bar graphs indicate the mean ± s.d. The dotted lines indicate the adherence of the relevant control to which all data were normalized. The control for **d** is 'parent'; the control for **e** is 'none'. Statistical comparisons were made by two-tailed Student's *t*-test: NS, not significant; $^*P < 0.05$; $^{***}P < 0.001$.

machinery may be reused (Fig. 2a and Supplementary Video 4). These frequent extension and retraction events allow for repetitive interactions of type IV competence pili with the extracellular environment. Using fluorescently labelled DNA, we also found that retracting type IV competence pili brought tip-bound DNA to the cell surface (Fig. 2c, Supplementary Fig. 7 and Supplementary Videos 5 and 6).

To determine whether pilus–DNA interactions were required for DNA uptake, we next sought to disrupt this interaction. Minor pilins can initiate pilus assembly and localize to the pilus tip[13,14], which we hypothesized could promote non-specific DNA binding[15] by ionic interactions. Consistent with this, we made targeted mutations of several positively charged residues within the major and minor pilins, and identified Arg/Lys mutations in two independent minor pilins (VC0858$^{R165Q}$ and VC0859$^{K148Q}$) that additively reduced DNA binding (Fig. 2d and Supplementary Fig. 5f,g) but did not substantially alter pilus dynamics (Supplementary Fig. 5a–c,h and Supplementary Video 7). These minor pilin mutants had significantly reduced rates of natural transformation (Fig. 2e) and DNA internalization (Fig. 2f), consistent with pilus–DNA interactions having an important role in DNA uptake. In addition, a distinct minor pilin point mutant (VC0858$^{R168Q}$) reduced DNA binding and natural transformation to the level of a *pilA* mutant (Supplementary Fig. 5d,e,g). Although this mutant produced as many pili as the *pilA*-Cys strain (Supplementary Fig. 5c), these pili displayed significantly altered pilus dynamics (Supplementary Fig. 5a,b,h and Supplementary Video 8). Despite this, many of the pilus events in the VC0858$^{R168Q}$ mutant were comparable to the rates of extension and retraction in the *pilA*-Cys strain (Supplementary Fig. 5a,b), which further supports that DNA binding is critical for DNA uptake.

Next, we assessed the spatiotemporal relationship between pilus dynamic activity and DNA internalization. As a marker for DNA uptake into the periplasm, we used a fluorescent fusion to ComEA, which is a critical competence protein that binds to DNA in the periplasm and results in the formation of readily observed foci upon DNA uptake[16–18], a finding that we recapitulate here (Supplementary Fig. 8). We found that an average of 14% of cells formed new ComEA foci in the presence of DNA, and that of those events, 64 ± 3% were immediately preceded by a retracting pilus at the same location (Fig. 3a,b and Supplementary Video 9). This value is probably an underestimate, as it does not account for short pili that cannot be resolved by light microscopy, pili occluded by the cell body or pili that may form outside the plane of focus. For the events where readily observed pilus retraction precedes DNA uptake, ComEA focus formation only occurred after what appears to be the completion of pilus retraction, which is consistent with DNA binding to the tip of type IV competence pili (Fig. 1a–c). The non-piliated *pilA* mutant formed no ComEA foci in either the presence or the absence of DNA (Fig. 3b). Thus, these data indicated that complete retraction of DNA-bound pili is required for DNA uptake.

To test this model further, we assessed whether retraction was required for DNA uptake. Because deletion of the gene encoding the retraction ATPase (*pilT*) alters the activity of type IV mannose-sensitive haemagglutinin (MSHA) pili[19] and may also have pleiotropic effects on gene expression[20], we tested this hypothesis more directly by sterically blocking type IV competence pilus retraction. This was accomplished by co-labelling *pilA*-Cys cells with EZ link biotin-PEG11-maleimide (biotin-mal) and AF488-mal before treating with neutravidin (a high-affinity biotin-binding protein), which specifically blocks the retraction of extended pili through the outer membrane secretin, probably by thickening the pilus fibre (Fig. 3c,d, Supplementary Fig. 9 and Supplementary Videos 10 and 11). Obstruction of pilus retraction resulted in an ~100-fold decrease in transformation frequency, indicating that at least ~99% of all DNA uptake events require the retraction of an extended pilus (Fig. 3e).

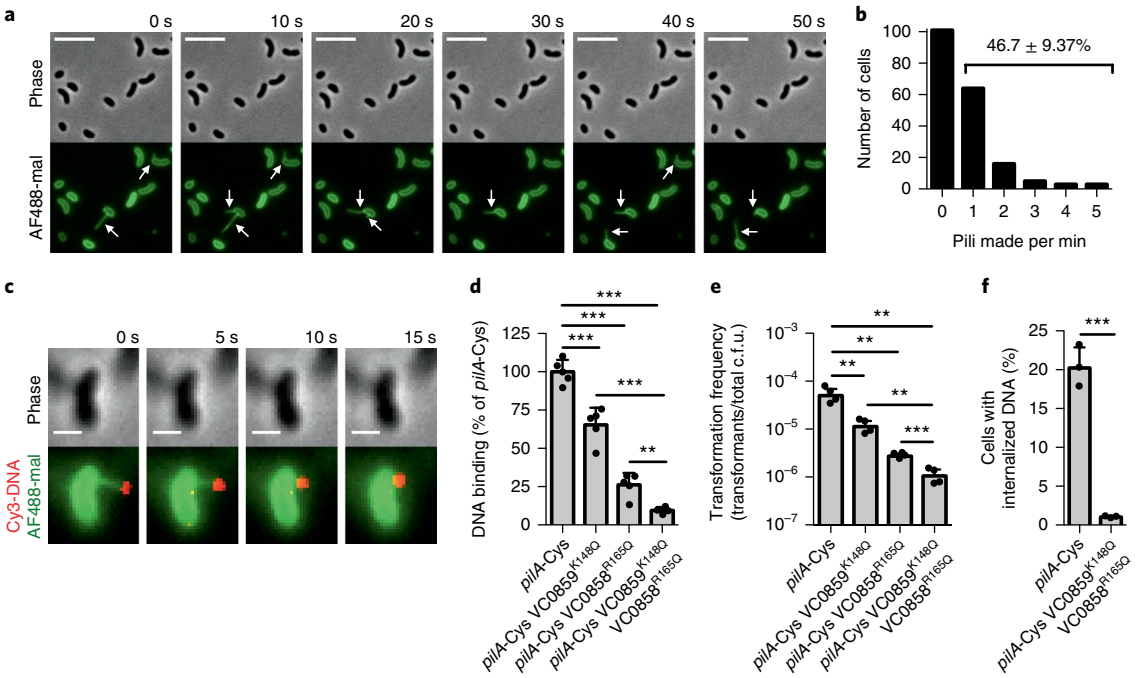


**Fig. 2 | Type IV competence pilus dynamic activity and DNA binding are critical for DNA internalization. a**, A montage of time-lapse imaging of *pilA*-Cys cells after labelling with the AF488-mal dye. The white arrows indicate pili. Scale bars, 5 μm. **b**, The number of cells making 0–5 pili within a 1-minute period. Data are from three independent biological replicates; $n = 192$ total pili observed. The percentage is the per cent of cells within the population that make pili within the 1-minute time frame ± s.d. **c**, A montage of time-lapse imaging of a retracting *pilA*-Cys strain after labelling with AF488-mal and incubation with fluorescently labelled DNA in a wet mount. Scale bars, 1 μm. Similar events were captured in three independent experiments. **d**, The relative DNA-binding assay of the indicated strains in Δ*pilT*-mutant backgrounds using a fluorescently labelled 6-kb PCR product. **e**, Natural transformation assays of the indicated strains. Cells were incubated with 5 ng of transforming DNA and DNase I was added to reactions after 10 minutes to prevent additional DNA uptake. **f**, DNA internalization assays of the indicated strains using a fluorescently labelled 6-kb PCR product. VC0858 and VC0859 encode minor pilins. Each data point in panels **d**–**f** represents an independent biological replicate ($n = 4$ for all samples (**d**,**e**); $n = 3$ for all samples (**f**)) and the bar graphs indicate the mean ± s.d. All statistical comparisons were made by two-tailed Student's *t*-test: $^{**}P$ 0.01; $^{***}P$ 0.001).

Furthermore, blocking pilus retraction resulted in very few DNA internalization events (Fig. 3b). Importantly, blocking pilus retraction using this approach did not inhibit binding to dsDNA (Supplementary Fig. 10). Recent work demonstrates that ComEA acts as a molecular ratchet to internalize DNA across the outer membrane, but it is currently unclear how DNA uptake is initiated because ComEA is localized to the periplasm[2,16,17]. Our results support a previously proposed model[21] in which ComEA-dependent internalization is initiated by the dynamic activity of DNA-binding type IV competence pili. Consistent with this, we found that DNA was not internalized in a *comEA* mutant despite this strain maintaining normal type IV competence pilus dynamic activity (Supplementary Fig. 11). Together, these results indicate that retraction of DNA-bound type IV competence pili initiates the process of DNA uptake into the periplasm during natural transformation, with concomitant uptake facilitated by ComEA-dependent molecular ratcheting.

Previous studies have shown that type IV pili require a PilT retraction ATPase to retract[22,23]. Contrary to this, we found that *pilT* mutants were still capable of retraction, as observed by correlated changes in cell body fluorescence that occurred upon extension and retraction of labelled pili during time-lapse experiments (Fig. 4a, Supplementary Fig. 12 and Supplementary Video 12). However, the *pilT* mutant exhibited a 10,000-fold reduction in transformation frequency and very little DNA internalization, despite exhibiting pilus retraction (Figs. 3b and 4a–d). Transformation of the Δ*pilT* mutant above the levels observed in the Δ*pilA* strain contrasts with a previous study[7], which may be the result of technical or strain differences (see Supplementary Discussion). Importantly, sterically blocking pili with biotin-mal and neutravidin, as discussed above, inhibited residual retraction events and transformation of the *pilT* mutant, indicating that retraction is still required for natural transformation in this background (Supplementary Fig. 13). We also found that PilT-independent natural transformation and retraction are not mediated by the PilT homologue PilU (Supplementary Fig. 14). Our data thus far indicate that tip-bound DNA is internalized via retraction through the outer membrane secretin pore. Thus, one possibility is that incomplete retraction in the *pilT* mutant may partially account for the highly reduced rate of transformation and DNA uptake observed.

DNA could be thread through the PilQ outer membrane secretin pore from one end or may undergo extreme bending to fit through this pore. We found that cells could internalize linear DNA and circular plasmids (that is, DNA lacking a free end) equally well (Supplementary Fig. 15), suggesting that DNA is probably bent when threaded across the membrane through PilQ. Because dsDNA has a persistence length of ~50 nm (or 150 bp), the extreme bending required to bring DNA through the relatively small PilQ pore (a diameter of 7–8 nm based on closely related systems)[24,25] would require a high force of retraction. Accordingly, another explanation for the lack of DNA uptake in *pilT* mutants may be a requirement for a high retraction force and speed to pull DNA through PilQ. To test whether the force and speed of retraction are altered in *pilT* mutants, we used a previously described micropillar assay in which cells use pili to bind to micropillars that bend as pilus retraction occurs, resulting in measurable retraction rates and forces[26]. The

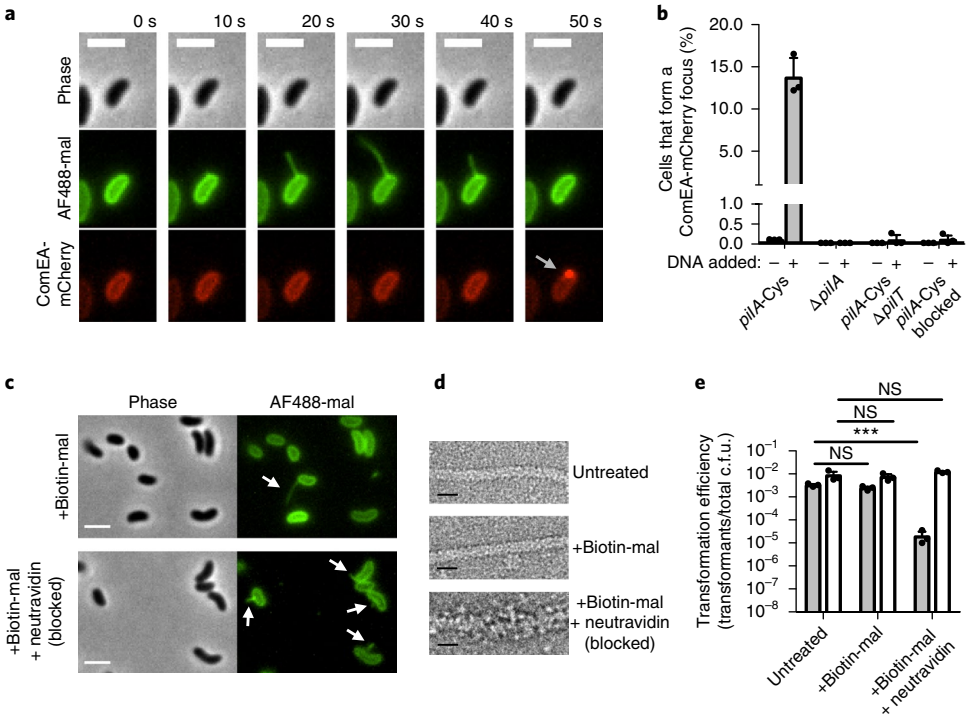


**Fig. 3 | Pilus retraction is required for DNA uptake. a**, A montage of time-lapse imaging of the *pilA*-Cys ComEA-mCherry strain labelled with AF488-mal showing ComEA focus formation after pilus retraction (grey arrow). Scale bars, 2 µm. **b**, The percentage of cells that formed a ComEA-mCherry focus within a 5-minute window in the presence or absence of DNA. Cells that had already formed ComEA-mCherry foci at the start of imaging were excluded from the analysis. Data are from three independent experiments ($n = 3$ for each condition) and shown as the mean ± s.d. **c**, Static images of *pilA*-Cys cells labelled with a 1:1 ratio of biotin-mal:AF488-mal with or without neutravidin. White arrows indicate pili. Scale bars, 2 µm. **d**, Transmission electron micrographs of *pilA*-Cys pili with the indicated treatments. Although untreated and biotin-mal-treated pili exhibit a similar thickness, the biotin-mal + neutravidin-treated pilus is approximately twice as thick. Scale bars, 10 nm. Images in panels **c** and **d** are representative of two independent experiments. **e**, Natural transformation assays of *pilA*-Cys (grey bars) or parent (white bars) strains after the indicated treatment. Cells were incubated with 500 ng of transforming DNA and DNase I was added to reactions after 10 minutes to prevent additional DNA uptake. Data are from three independent biological replicates and shown as the mean ± s.d. Statistical comparisons were made by two-tailed Student's *t*-test: NS, not significant; ***$P < 0.001$.

*pilT* mutant exhibited a significant reduction in both the speed and the force of retraction (Fig. 4c,d). Consequently, reduced transformation in the *pilT* mutant may be explained by either a lack of full retraction and/or a reduction in the force or speed of retraction, which prevents translocation of DNA across the outer membrane. Coupled with recent reports that divergent pili lacking a *pilT* homologue can retract[8,13], these data support a model in which *pilT*-independent retraction may be conserved across diverse systems, including competence pili from species that lack defined pilus retraction machinery (for example, *Streptococcus pneumoniae*, *Bacillus subtilis* and *Haemophilus influenzae*). However, whether additional canonical type IV pili also exhibit PilT-independent retraction remains to be seen.

The binding and transport of large DNA molecules across the cell envelope is critical for horizontal gene transfer in diverse microbial species, and DNA taken up during this process can also be used as a nutrient. Here, we clarify the mechanism of action for type IV competence pili, which are the complex nanomachines that promote DNA uptake during natural transformation (Fig. 4e). DNA uptake in *V. cholerae* is sequence independent[15], and we show that minor pilins probably promote DNA binding at the pilus tip. DNA binding to pili in *Neisseria* is also mediated by a minor pilin, ComP, which binds to a species-specific DNA uptake sequence[27,28]. Despite minor pilins having a role in DNA binding in both of these systems, the proteins involved lack homology, suggesting that distinct mechanisms for pilus–DNA binding probably exist among diverse competence pilus systems.

The binding of DNA to the pilus tip as observed here is also compelling because the secretin pore through which the pilus extends and retracts is only wide enough to accommodate the pilus fibre and would probably exclude DNA bound along the pilus length[24,25]. Thus, retraction of tip-bound DNA could allow for the threading of DNA through the secretin pore in the wake of a retracting pilus fibre. However, our data indicate that pilus retraction is not sufficient for DNA uptake into the periplasm, but probably works in conjunction with the molecular ratchet ComEA[2,17] to mediate efficient DNA uptake.

We show that type IV competence pili in *V. cholerae* exhibit different rates of extension and retraction, which contrasts with other type IV pilus systems that have been characterized in which the rates of extension and retraction are equal[8,29]. Notably, the speed of extension and/or retraction were markedly slower than the rates observed for other canonical type IV pili as in *Neisseria gonorrhoeae* (retraction: ~1.2 µm $s^{-1}$ (ref. [30])) and *Pseudomonas aeruginosa* (extension and retraction: ~0.5 µm $s^{-1}$ (ref. [29])). The mechanism underlying this difference is unclear; however, the pilus from *V. cholerae* studied here is largely dedicated to competence, whereas the pili in *N. gonorrhoeae* and *P. aeruginosa* can mediate twitching motility, which could account for this difference.

Although the type IV competence pili of *V. cholerae* studied here are long micrometre-scale surface appendages, many naturally competent species (such as *B. subtilis* and *H. influenzae*) possess short 'pseudopili' that are thought to simply span the cell envelope. However, both long competence pili and short pseudopili could

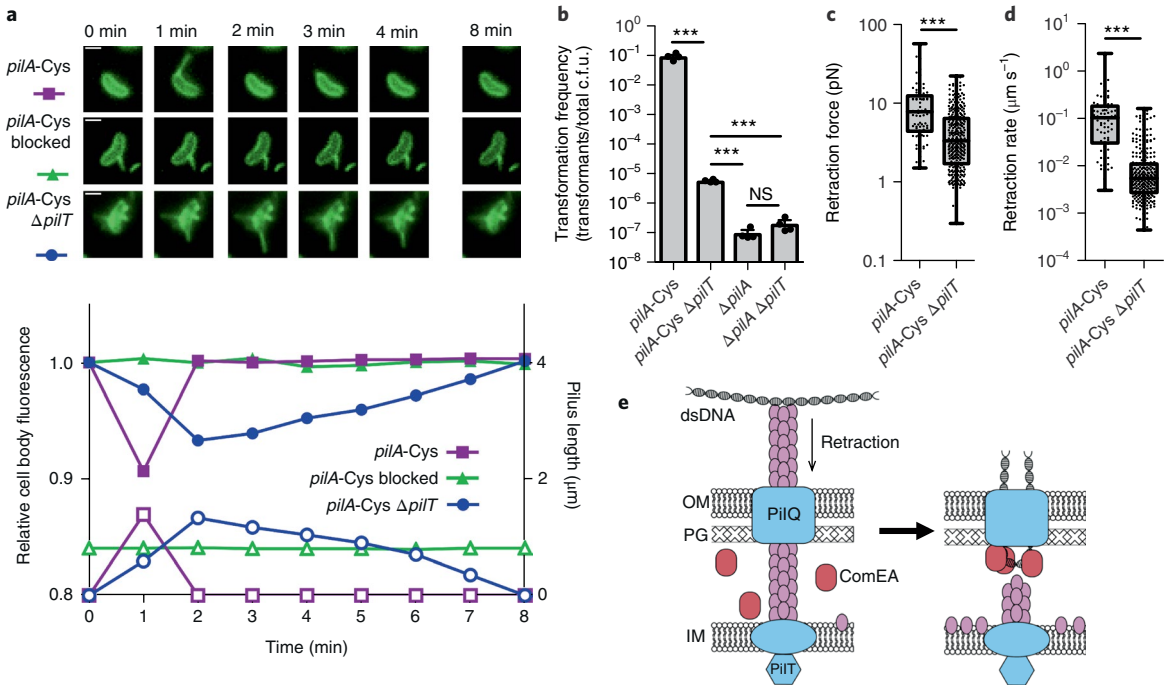


**Fig. 4 | Residual retraction in Δ*pilT* mutants allows for low rates of transformation. a**, A montage (top) of cells measured for corresponding plots (bottom) showing the relative cell body fluorescence (closed symbols) and the correlated pilus length (open symbols) over time for *pilA*-Cys labelled with AF488-mal (squares), *pilA*-Cys blocked for retraction by labelling with a 1:1 ratio of biotin-mal:AF488-mal and neutravidin (triangles) or *pilA*-Cys Δ*pilT* labelled with AF488-mal (circles). Scale bars, 1 μm. Data are representative of three independent experiments. **b**, Natural transformation assays of the indicated strains using 500 ng of transforming DNA. Data are from four independent biological replicates and shown as the mean ± s.d. **c**,**d**, Micropillar assays were performed with the indicated strains to measure the retraction force (*pilA*-Cys: $n = 79$, *pilA*-Cys Δ*pilT*: $n = 339$) (**c**) and the retraction speed (*pilA*-Cys: $n = 76$; *pilA*-Cys Δ*pilT*: $n = 288$) (**d**). Box plots indicate the median and the first and third quartiles, while the whiskers denote the range. Each data point in the overlay for panels **c** and **d** represents an independent retraction event. Statistical comparisons in panels **b**–**d** were made by two-tailed Student's *t*-test: NS, not significant; ***$P$ 0.001. **e**, A model of pilus retraction-mediated DNA uptake. Retraction of DNA-bound pili threads dsDNA across the outer membrane (OM; left) followed by ComEA-dependent molecular ratcheting (right) to promote uptake. IM, inner membrane; PG, peptidoglycan.

engage in DNA uptake through a similar mechanism by binding to DNA via their exposed tip and using retraction to pull bound DNA through the outer membrane in Gram-negative species or to pull this DNA through the thick peptidoglycan layer in Gram-positive species. Long extended pili involved in competence (as in *V. cholerae*, *Neisseria* spp., *S. pneumoniae* and *Acinetobacter baylyi*) may not be critical for the recruitment of freely diffusible DNA (as short pseudopili would suffice), but instead, these structures may be important for binding to and the uptake of DNA bound to surfaces, as would probably be the case in bacterial biofilms.

## Methods

**Bacterial strains and culture conditions.** All *V. cholerae* strains used throughout this study are derivatives of the El Tor isolate E7946 (ref. [31]). Competence induction in *V. cholerae* requires two cues: chitin oligosaccharides and quorum sensing, which activate the expression of TfoX and HapR, respectively[6,32–34]. Thus, to constitutively activate competence, we ectopically expressed TfoX (via $P_{tac}$-*tfoX*) and constitutively activated quorum sensing via inactivation of *luxO*[35,36]. For a list of all strains used throughout this study, see Supplementary Table 1. Bacteria were routinely cultivated on LB Miller broth and agar supplemented with kanamycin (50 μg ml$^{-1}$), spectinomycin (200 μg ml$^{-1}$), trimethoprim (10 μg ml$^{-1}$), chloramphenicol (1 μg ml$^{-1}$), erythromycin (10 μg ml$^{-1}$), carbenicillin (100 μg ml$^{-1}$) and/or zeocin (50 μg ml$^{-1}$) as appropriate. Instant ocean medium (7 g l$^{-1}$; Aquarium Systems) was used throughout the study where indicated.

**Construction of mutant strains.** Mutants were constructed by MuGENT, Exo-MuGENT and/or natural transformation exactly as previously described[35,37]. Briefly, mutant constructs for deletions or fluorescent fusions were generated via splicing-by-overlap PCR to stitch (1) the upstream region of homology (aka the UP arm), (2) the mutation (aka the MIDDLE arm, which could represent an antibiotic resistance cassette or a fluorescent gene) and (3) the downstream region of homology (aka the DOWN arm). For a list of primers used to generate all mutant constructs, see Supplementary Table 2. The UP arm was amplified via an F1/R1 primer pair, whereas the DOWN arm was amplified with the F2/R2 primer pair. All antibiotic resistance cassettes were amplified with ABD123 (ATTCCGGGGATCCGTCGAC) and ABD124 (TGTAGGCTGGAGCTGCTTC). Fluorescent genes were amplified with the primers indicated in Supplementary Table 2. Splicing-by-overlap PCR reactions were carried out using a mixture of the UP, MIDDLE and DOWN arms in a PCR reaction as a template with the F1 and R2 primers. These constructs were then introduced into naturally competent strains (for products with an antibiotic resistance marker), as described below in 'Natural transformation assays', or by co-transformation (for constructs like fluorescent fusions, which lack a resistance marker) as previously described[35].

For point mutations, mutant constructs were generated via a single PCR reaction using an allele-specific F primer that contained >35 bp of homology upstream of the point mutation and an R2 primer to generate the downstream region of homology. This product was introduced into a *recJ exoVII* mutant of *V. cholerae* via co-transformation as previously described[37]. Subsequently, point mutations were amplified off of the genomic DNA of these strains with F1/R2 primers and then transferred to strains of interest by co-transformation[35].

Mutants were confirmed by PCR and/or sequencing. The $P_{tac}$-*tfoX* and Δ*lacZ*::*lacIq* mutant constructs are from a previously published study[35]. To design Cys replacement mutants and minor pilin Lys/Arg mutations, amino acid residues from pilin sequences were analysed for solvent accessibility, as described previously[8], using solvent accessibility prediction software[38].

**Natural transformation assays.** Chitin-dependent and chitin-independent transformation assays were conducted as previously described[35,37]. Unless otherwise noted, natural transformation assays were chitin independent using strains containing isopropyl-β-D-thiogalactoside (IPTG)-inducible $P_{tac}$-*tfoX* and Δ*luxO* mutations to induce competence. For chitin-independent transformation assays, the indicated strains were grown to the late-log phase in LB + 100 μM IPTG (to induce TfoX expression) + 20 mM $MgCl_2$ + 10 mM $CaCl_2$. Then, ~$10^8$ c.f.u. (colony-forming unit) of this culture were diluted into instant ocean medium. Next, ~500 ng transforming DNA were added to each reaction and allowed to incubate for an additional 5 h at 30 °C to allow for natural transformation. For each strain tested, negative controls were performed where no DNA was added.

VC1807 is a frame-shifted transposase and its mutation does not impact the growth of *V. cholerae*[35]; thus, PCR products for ΔVC1807::Ab$^R$ (Ab$^R$ = Cm$^R$, Zeo$^R$, Tm$^R$ or Erm$^R$ resistance cassettes depending on the resistance profiles of the strains tested) containing 3-kb homology arms (required for the maximum rates of transformation[35]) were used to test transformation frequency throughout this article. Next, reactions were outgrown by the addition of 1 ml LB and shaking at 37 °C for 2 h followed by plating on media to select for transformants (that is, media to select for the integration of ΔVC1807::Ab$^R$) and on non-selective media to assess the total viable counts. Transformation frequency was defined as the number of transformants divided by the total viable counts. Where indicated, 25 μg ml$^{-1}$ AF488-mal (Thermo Fisher) was added to the chitin-independent transformation assays 15 min before the addition of transforming DNA.

For chitin-dependent natural transformation assays (only used in Supplementary Fig. 1c), ~$10^8$ c.f.u. of a mid-log culture of the indicated strain were incubated on chitin powder from shrimp cells (Alfa Aesar) in instant ocean medium for 24 h to allow for competence induction. Then, 500 ng ΔVC1807::Ab$^R$ transforming DNA were added, and reactions were incubated, outgrown and plated exactly as described above for chitin-independent transformation assays to attain the transformation frequency.

For co-transformation assays, cells were incubated with two genetically unlinked markers. One marker was a ΔVC1807::Erm$^R$ mutant construct, whereas the other marker was a previously described ΔVCA1045 mutant construct[39], which inactivates the sole mannitol transporter in *V. cholerae*. In these assays, 10 ng ΔVC1807::Erm$^R$ PCR product were added to the transformation assays and then ~3 μg ΔVCA1045 PCR product were either added to cells immediately or after a 3-h delay. Cells were then outgrown and plated onto Erm-containing media to select for integration of the ΔVC1807::Erm$^R$ product. Twenty-four colonies were then patched into M9 minimal medium containing mannitol as a sole carbon source to screen for integration of the ΔVCA1045 mutant construct. The co-transformation frequency was defined as the percentage of the ΔVC1807::Erm$^R$ mutants that incorporated the ΔVCA1045 product.

To physically obstruct pilus retraction, ~$10^8$ c.f.u. of the indicated strains grown to the late-log phase under competence-inducing conditions were washed in instant ocean medium and incubated with 50 μg ml$^{-1}$ biotin-mal (Thermo Fisher) for 45 min at room temperature. Then, cells were pelleted and washed twice in instant ocean medium. Next, ~$10^7$ c.f.u. were diluted into fresh instant ocean medium. Where indicated, neutravidin (Thermo Fisher) was then added to reactions at a final concentration of 1.32 mg ml$^{-1}$ and incubated at room temperature for 30 min. Then, 500 ng ΔVC1807::Ab$^R$ transforming DNA were added and reactions were incubated at 30 °C. For strains where *pilT* was intact, reactions were allowed to proceed for 10 min before the addition of 10 units of DNAse I (NEB) to prevent additional DNA uptake. This was performed because the production of new pilins during the normal 5-h DNA incubation would circumvent our method to block pilus retraction. For transformation assays in the Δ*pilT* mutant background, a 10-min incubation with DNA was insufficient to obtain any transformants. Thus, reactions were allowed to proceed for 1 h at 30 °C prior to the addition of DNAse I as described above. Following DNA addition, all reactions were incubated at 30 °C for a total of 5 h (regardless of the time of DNAse I addition) to allow for DNA integration. Reactions were then outgrown and plated exactly as described above to attain the transformation frequency.

For natural transformation assays of minor pilin DNA-binding mutants, strains were incubated with 5 ng ΔVC1807::Ab$^R$ transforming DNA. After 5 mins, DNAse I was added to prevent additional DNA uptake, and reactions were then outgrown and plated as described above. This was performed to sensitize the assay to the effects of DNA binding on natural transformation.

**Pilin labelling, imaging and quantification.** Pilin labelling was achieved using AF488-mal. Cultures were grown to the late-log phase in LB supplemented with 20 mM $MgCl_2$, 10 mM $CaCl_2$ and 100 μM IPTG to induce competence. Approximately $10^8$ c.f.u. were then centrifuged at 16,000*g* for 1 min and then resuspended in instant ocean medium supplemented with 20 mM $MgCl_2$ and 10 mM $CaCl_2$ before labelling with 25 μg ml$^{-1}$ AF488-mal for 30 min. Labelled cells were centrifuged, washed once and resuspended in instant ocean medium. Cell bodies were imaged using phase-contrast microscopy, whereas labelled pili were imaged using fluorescence microscopy on a Nikon Ti-2 microscope using a Plan Apo ×60 objective, a green fluorescent protein or DsRed filter cube, a Hamamatsu ORCAFlash4.0 camera and Nikon NIS Elements imaging software. Cell numbers were quantified using MicrobeJ[40]. To determine pilus length and the rates of extension and retraction, labelled cells were imaged by time-lapse microscopy every second for 1 min. For pilus length measurements, pili that were already retracting when imaging began were excluded from the analysis. For extension and retraction rate calculations, only cells that made a single pilus that began extension and fully retracted within the 1-min window were analysed. To determine the number of pili made per cell, the per cent of cells that make pili and the per cent of cells that form a ComEA-mCherry focus, labelled cells were imaged in the presence or absence of 1 μg DNA by time-lapse microscopy every 10 s for 5 min. Pilus length, extension and retraction rates, the number of pili made per cell, the per cent of cells that make pili and the per cent of cells that form a ComEA-mCherry focus were manually calculated using measurement tools of the NIS Elements analysis software. To block pilus retraction for fluorescence microscopy, cells were co-labelled with 25 μg ml$^{-1}$ AF488-mal and 25 μg ml$^{-1}$ biotin-mal for 30 min before washing. Where indicated, 1.32 mg ml$^{-1}$ neutravidin was then added to washed cells and incubated for 30 min at room temperature before imaging. All imaging was performed under 0.2% Gelzan (Sigma) pads made with instant ocean medium.

**Fluorescent DNA-binding and localization assays.** Strains used for DNA-binding and localization assays contained Δ*pilT* mutations to ensure the presence of extended pili for DNA binding and to diminish DNA uptake. Fluorescently labelled Cy3-DNA and MFP488-DNA were generated using a 6-kb ΔVC1807::Ab$^R$ PCR product (the same product used for the transformation efficiency assays throughout this article) and the LabelIT kit (Mirus Biosciences), which covalently adds a fluorescent label onto ~1 in every 20–60 bp. For DNA-binding assays, the indicated strains were grown to the late-log phase in LB + 100 μM IPTG + 20 mM $MgCl_2$ + 10 mM $CaCl_2$. Then, ~$10^8$ c.f.u. were centrifuged and washed in instant ocean medium. Cells were then incubated with 100 ng Cy3-labelled or MFP488-labelled DNA at room temperature for 15 min (MFP488-labelled DNA was used for DNA pulldowns of minor pilin mutant strains because they contained *comEA*-mCherry, which has substantial spectral overlap with Cy3). Cells were then pelleted and washed twice with fresh instant ocean to remove unbound DNA. Reactions were then transferred to a 96-well plate, and Cy3 or MFP488 fluorescence was determined on a Biotek H1M plate reader. Where indicated, 5 μg ssDNA (PhiX virion DNA; NEB), 5 μg dsDNA (PhiX RFII DNA; NEB) or 10 μg acetylated BSA (Promega) were added to DNA-binding reactions as non-labelled competitors. Where indicated, strains were labelled with biotin-mal and/or neutravidin exactly as described above for the natural transformation assays.

For microscopy localization assays on cell-associated pili, cells were labelled as described above before they were added to a coverslip with BSA (0.2 mg ml$^{-1}$) and 4 ng Cy3-labelled DNA. After incubation for 5–15 min, cells were imaged using a Cy3 filter cube every 3 s for 2 min. During imaging, we noticed that the majority of DNA-binding events occurred at the ends of pilus fibres. However, we experienced several limitations using this setup that prevented quantitative analysis. For example, the large number of pili in the Δ*pilT* mutants obscured how many fibres were binding DNA puncta, the cell body fluorescence prevented observation of DNA binding to pili shorter than 1 μm, and Brownian motion in this setup resulted in pili and DNA movement outside of the focal plane.

For robust quantification of DNA localization along pilus filaments, we used sheared pili bound to surfaces within microfluidic channels to alleviate the limitations of using cell-associated pili and to further demonstrate that DNA binding was pilus dependent. Microfluidic channel devices were constructed exactly as described previously[8]. Channels were pre-treated with BSA (0.2 mg ml$^{-1}$) in instant ocean medium to reduce nonspecific adherence. Then, ~$10^8$ AF488-mal-labelled cells were vortexed to shear pili and then cells and sheared pili were added to microchannels and incubated for 30 min at room temperature to allow for pilus attachment to the microfluidic channel surfaces. Next, 11 ng Cy3-labelled DNA in a total volume of 400 μl instant ocean medium were added to the channel to both flush away unattached cells and pili and to introduce DNA to the microchannel. Then, the chamber was incubated at room temperature for 5–15 min with DNA to allow for DNA–pilus association before imaging. To confirm DNA–pilus binding, gravity flow was applied to microfluidic channels by altering the heights of the input and output tubing to bring both pili and bound DNA into the same field of view for imaging. Only DNA molecules that exhibited co-localization with pili during flow directional changes were analysed, allowing for the exclusion of glass-bound DNA from the analysis. Pili shorter than 0.5 μm were excluded from the analysis as their movement could not be resolved with directional flow changes. Pilus length and DNA localization were determined using MicrobeJ[32]. Pilus lengths were normalized where the glass-bound end was fixed at 0 and the free end was 1.0, and the relative DNA binding was then plotted along the normalized length.

To observe type IV competence pili pulling fluorescent DNA, *pilA*-Cys cells harbouring native *comEA* (TND0651) were grown to the late-log phase in LB + 100 μM IPTG + 20 mM $MgCl_2$ + 10 mM $CaCl_2$, washed in instant ocean and then mixed with ~5 ng Cy3-labelled DNA and acetylated BSA was added to 100 μg ml$^{-1}$. Next, a wet mount was prepared for microscopy on an inverted scope by placing 5–10 μl of sample onto a 22 × 50-mm coverslip and then covering the sample with a 22 × 22-mm coverslip. Time-lapse imaging was then performed as described above.

**DNA internalization assay.** Approximately $10^8$ c.f.u. of cells grown to the late-log phase in LB + 100 μM IPTG + 20 mM $MgCl_2$ + 10 mM $CaCl_2$ were pelleted and resuspended in instant ocean medium. Cells were then incubated with 10 ng of either an MFP488-labelled 6-kb ΔVC1807::Ab$^R$ PCR product or an ~6-kb supercoiled plasmid (pBAD18Kan) at room temperature for 1 h. Next, 10 units of DNase I was added to reactions and incubated at room temperature for 1 min to degrade any remaining extracellular DNA. Cells were then washed once with instant ocean medium to remove excess dye and imaged. The percentage of cells with internalized DNA was quantified using MicrobeJ.

**mCherry-PilQ localization.** Cells were grown to the late-log phase in LB + 100 μM IPTG + 20 mM $MgCl_2$ + 10 mM $CaCl_2$ and imaged. Localization of mCherry-PilQ foci was determined and plotted using MicrobeJ.

**Cell body fluorescence quantification.** Strains were labelled with AF488-mal as indicated above and imaged for 10-s intervals over a 20-min window. Integrated fluorescence intensity was measured for both the cell body and the pilus for each cell for each time point using ImageJ[41]. Fluorescence intensities were normalized for photobleaching over the time-lapse experiment by multiplying the measured fluorescence intensity by the percentage of fluorescence lost from the total fluorescence intensity (the sum of the cell body and the pilus intensities) for each time point. After adjustment for photobleaching, the cell body fluorescence for each time point was divided by the cell body fluorescence measured at time 0. The relative cell body intensity changes were plotted with the measured pilus length for each time point.

**Negative-stain electron microscopy.** To ensure that the pili imaged via electron microscopy were type IV competence pili, we inactivated the two other type IV pilus systems (MSHA and toxin-coregulated pili (TCP)) in *V. cholerae*, yielding strain SAD2094 (see Supplementary Table 1 for additional strain details). We also generated a *pilA*-Cys mutation in this background (SAD2093). Strains were grown to the late-log phase in LB + 100 μM IPTG + 20 mM $MgCl_2$ + 10 mM $CaCl_2$ and then treated with biotin-mal and/or neutravidin exactly as described above for the natural transformation assays.

To prepare the negative-stain specimen, 4 μl sample solution was applied on a glow-discharged, carbon-coated, 300-mesh copper grid for 30 s. The excess solution was removed by a piece of filter paper. The grid was washed with 4 μl Milli-Q water, stained with 4 μl of 0.75% (w/v) uranyl formate for 25 s and blotted to dry. The images were acquired at a nominal magnification of ×10,000, ×20,000 or ×40,000 using the JEOL JEM-1400 Plus transmission electron microscope operated at 120 kV and a Gatan 4k x 4k OneView Camera.

**Micropillar retraction assay.** To ensure that all measurements recorded were due to type IV competence pili, all the experiments were performed with strains lacking all external appendages other than type IV competence pili as well as exopolysaccharide production (that is, mutants lacking flagella, MSHA pili, TCP pili and *Vibrio* polysaccharide (VPS) production). See Supplementary Table 1 for additional strain details. Strains were grown overnight in LB either directly from frozen stocks or from a single colony off of an LB agar plate. Of the overnight liquid culture, 50 μl was subcultured into 3 ml LB + 100 μM IPTG + 20 mM $MgCl_2$ + 10 mM $CaCl_2$ and allowed to grow at 30 °C for 5 h. Then, 100 μl of this culture was centrifuged for 5 min at 20,000*g* and the bacteria were resuspended in instant ocean medium. At different times, 10 μl of the resuspension were added to micropillars in an observation chamber as previously reported[26]. Briefly, silica molds were inverted on activated coverslips with polyacrylamide gels in between. The result is an array of flexible micropillars in a hexagonal array of 3 μm × 3 μm. Once the bacteria were in contact with the micropillars, 10-Hz movies of the top of the pillars were recorded. The motion of the tips of the pillars was tracked using a cross-correlation algorithm in ImageJ[41]. The amplitude and speeds of the pillars' motions were then analysed using MATLAB. Finally, we calibrated the pillars' stiffness constant using optical tweezers as previously described[26]. The pillars used in this study have a stiffness constant of $17 \pm 4$ pN μm$^{-1}$.

**Statistics.** Significance was calculated using statistical tests on the GraphPad (Prism) 5.0 software. Statistical differences between two groups were analysed using two-tailed Student's *t*-tests. Complete statistics can be found in Supplementary Table 3. Sample sizes were chosen based on historical data and no statistical methods were used to predetermine sample size.

**Reporting Summary.** Further information on experimental design is available in the Nature Research Reporting Summary linked to this article.

**Data availability.** The data that support the findings of this study are available from the corresponding author upon request.

Received: 26 February 2018; Accepted: 10 May 2018;
Published online: 11 June 2018

## References

1. Chen, I. & Dubnau, D. DNA uptake during bacterial transformation. *Nat. Rev. Microbiol.* **2**, 241–249 (2004).
2. Hepp, C. & Maier, B. Kinetics of DNA uptake during transformation provide evidence for a translocation ratchet mechanism. *Proc. Natl Acad. Sci. USA* **113**, 12467–12472 (2016).
3. Muschiol, S., Balaban, M., Normark, S. & Henriques-Normark, B. Uptake of extracellular DNA: competence induced pili in natural transformation of *Streptococcus pneumoniae*. *Bioessays* **37**, 426–435 (2015).
4. Graupner, S., Weger, N., Sohni, M. & Wackernagel, W. Requirement of novel competence genes *pilT* and *pilU* of *Pseudomonas stutzeri* for natural transformation and suppression of *pilT* deficiency by a hexahistidine tag on the type IV pilus protein PilAI. *J. Bacteriol.* **183**, 4694–4701 (2001).
5. Laurenceau, R. et al. A type IV pilus mediates DNA binding during natural transformation in *Streptococcus pneumoniae*. *PLoS Pathog.* **9**, e1003473 (2013).
6. Meibom, K. L., Blokesch, M., Dolganov, N. A., Wu, C. Y. & Schoolnik, G. K. Chitin induces natural competence in *Vibrio cholerae*. *Science* **310**, 1824–1827 (2005).
7. Seitz, P. & Blokesch, M. DNA-uptake machinery of naturally competent *Vibrio cholerae*. *Proc. Natl Acad. Sci. USA* **110**, 17987–17992 (2013).
8. Ellison, C. K. et al. Obstruction of pilus retraction stimulates bacterial surface sensing. *Science* **358**, 535–538 (2017).
9. Hepp, C., Gangel, H., Henseler, K., Gunther, N. & Maier, B. Single-stranded DNA uptake during gonococcal transformation. *J. Bacteriol.* **198**, 2515–2523 (2016).
10. Duffin, P. M. & Seifert, H. S. Genetic transformation of *Neisseria gonorrhoeae* shows a strand preference. *FEMS Microbiol. Lett.* **334**, 44–48 (2012).
11. Assalkhou, R. et al. The outer membrane secretin PilQ from *Neisseria meningitidis* binds DNA. *Microbiology* **153**, 1593–1603 (2007).
12. Burkhardt, J., Vonck, J. & Averhoff, B. Structure and function of PilQ, a secretin of the DNA transporter from the thermophilic bacterium *Thermus thermophilus* HB27. *J. Biol. Chem.* **286**, 9977–9984 (2011).
13. Ng, D. et al. The *Vibrio cholerae* minor pilin TcpB initiates assembly and retraction of the toxin-coregulated pilus. *PLoS Pathog.* **12**, e1006109 (2016).
14. Nguyen, Y. et al. *Pseudomonas aeruginosa* minor pilins prime type IVa pilus assembly and promote surface display of the PilY1 adhesin. *J. Biol. Chem.* **290**, 601–611 (2015).
15. Suckow, G., Seitz, P. & Blokesch, M. Quorum sensing contributes to natural transformation of *Vibrio cholerae* in a species-specific manner. *J. Bacteriol.* **193**, 4914–4924 (2011).
16. Gangel, H. et al. Concerted spatio-temporal dynamics of imported DNA and ComE DNA uptake protein during gonococcal transformation. *PLoS Pathog.* **10**, e1004043 (2014).
17. Seitz, P. et al. ComEA is essential for the transfer of external DNA into the periplasm in naturally transformable *Vibrio cholerae* cells. *PLoS Genet.* **10**, e1004066 (2014).
18. Borgeaud, S., Metzger, L. C., Scrignari, T. & Blokesch, M. The type VI secretion system of *Vibrio cholerae* fosters horizontal gene transfer. *Science* **347**, 63–67 (2015).
19. Watnick, P. I. & Kolter, R. Steps in the development of a *Vibrio cholerae* El Tor biofilm. *Mol. Microbiol.* **34**, 586–595 (1999).
20. Dietrich, M., Mollenkopf, H., So, M. & Friedrich, A. Pilin regulation in the *pilT* mutant of *Neisseria gonorrhoeae* strain MS11. *FEMS Microbiol. Lett.* **296**, 248–256 (2009).
21. Hepp, C. & Maier, B. Bacterial translocation ratchets: shared physical principles with different molecular implementations: how bacterial secretion systems bias Brownian motion for efficient translocation of macromolecules. *Bioessays* **39**, e201700099 (2017).
22. Burrows, L. L. *Pseudomonas aeruginosa* twitching motility: type IV pili in action. *Annu. Rev. Microbiol.* **66**, 493–520 (2012).
23. Craig, L., Pique, M. E. & Tainer, J. A. Type IV pilus structure and bacterial pathogenicity. *Nat. Rev. Microbiol.* **2**, 363–378 (2004).
24. Chang, Y. W. et al. Architecture of the type IVa pilus machine. *Science* **351**, aad2001 (2016).
25. Gold, V. A., Salzer, R., Averhoff, B. & Kuhlbrandt, W. Structure of a type IV pilus machinery in the open and closed state. *eLife* **4**, e07380 (2015).
26. Biais, N., Higashi, D., So, M. & Ladoux, B. Techniques to measure pilus retraction forces. *Methods Mol. Biol.* **799**, 197–216 (2012).
27. Cehovin, A. et al. Specific DNA recognition mediated by a type IV pilin. *Proc. Natl Acad. Sci. USA* **110**, 3065–3070 (2013).
28. Berry, J. L. et al. A comparative structure/function analysis of two type IV pilin DNA receptors defines a novel mode of DNA binding. *Structure* **24**, 926–934 (2016).
29. Skerker, J. M. & Berg, H. C. Direct observation of extension and retraction of type IV pili. *Proc. Natl Acad. Sci. USA* **98**, 6901–6904 (2001).
30. Maier, B. et al. Single pilus motor forces exceed 100 pN. *Proc. Natl Acad. Sci. USA* **99**, 16012–16017 (2002).
31. Miller, V. L., DiRita, V. J. & Mekalanos, J. J. Identification of *toxS*, a regulatory gene whose product enhances ToxR-mediated activation of the cholera toxin promoter. *J. Bacteriol.* **171**, 1288–1293 (1989).
32. Dalia, A. B., Lazinski, D. W. & Camilli, A. Identification of a membrane-bound transcriptional regulator that links chitin and natural competence in *Vibrio cholerae*. *mBio* **5**, e01028-13 (2014).
33. Lo Scrudato, M. & Blokesch, M. The regulatory network of natural competence and transformation of *Vibrio cholerae*. *PLoS Genet.* **8**, e1002778 (2012).
34. Lo Scrudato, M. & Blokesch, M. A transcriptional regulator linking quorum sensing and chitin induction to render *Vibrio cholerae* naturally transformable. *Nucleic Acids Res.* **41**, 3644–3658 (2013).
35. Dalia, A. B., McDonough, E. & Camilli, A. Multiplex genome editing by natural transformation. *Proc. Natl Acad. Sci. USA* **111**, 8937–8942 (2014).

36. Zhu, J. et al. Quorum-sensing regulators control virulence gene expression in *Vibrio cholerae*. *Proc. Natl Acad. Sci. USA* **99**, 3129–3134 (2002).
37. Dalia, T. N. et al. Enhancing multiplex genome editing by natural transformation (MuGENT) via inactivation of ssDNA exonucleases. *Nucleic Acids Res.* **45**, 7527–7537 (2017).
38. Petersen, B., Petersen, T. N., Andersen, P., Nielsen, M. & Lundegaard, C. A generic method for assignment of reliability scores applied to solvent accessibility predictions. *BMC Struct. Biol.* **9**, 51 (2009).
39. Hayes, C. A., Dalia, T. N. & Dalia, A. B. Systematic genetic dissection of PTS in *Vibrio cholerae* uncovers a novel glucose transporter and a limited role for PTS during infection of a mammalian host. *Mol. Microbiol.* **104**, 568–579 (2017).
40. Ducret, A., Quardokus, E. M. & Brun, Y. V. MicrobeJ, a tool for high throughput bacterial cell detection and quantitative analysis. *Nat. Microbiol.* **1**, 16077 (2016).
41. Collins, T. J. ImageJ for microscopy. *Biotechniques* **43**, 25–30 (2007).

## Acknowledgements

We thank A. Camilli, F. Yildiz, D. Kearns, N. Greene, C. Berne and B. LaSarre for critical comments on the manuscript. We also thank members of the Biais lab, L. Khosla, R. Rayyan and A. Ratkiewicz for assistance with micropillar assays. This work was supported by grant R35GM122556 from the National Institutes of Health to Y.V.B., by grant AI118863 from the National Institutes of Health to A.B.D., by the National Science Foundation fellowship 1342962 to C.K.E. and by grant AI116566 from the National Institutes of Health to N.B.

## Author contributions

C.K.E. and A.B.D. designed and coordinated the overall study. A.B.D., C.K.E., T.N.D., J.C.-Y.W., A.V.C. and N.B. performed the experiments. Y.V.B., A.B.D., C.K.E., T.N.D. and N.B. analysed and interpreted the data. C.K.E. and A.B.D. wrote the manuscript with help from Y.V.B.

## Competing interests

The authors declare no competing interests.

## Additional information

**Supplementary information** is available for this paper at https://doi.org/10.1038/s41564-018-0174-y.

**Reprints and permissions information** is available at www.nature.com/reprints.

**Correspondence and requests for materials** should be addressed to A.B.D.

nature research

Corresponding author(s): Ankur Dalia

# Reporting Summary

Nature Research wishes to improve the reproducibility of the work that we publish. This form provides structure for consistency and transparency in reporting. For further information on Nature Research policies, see Authors & Referees and the Editorial Policy Checklist.

## Statistical parameters

When statistical analyses are reported, confirm that the following items are present in the relevant location (e.g. figure legend, table legend, main text, or Methods section).

| n/a | Confirmed | |
|---|---|---|
| ☐ | ☒ | The exact sample size (*n*) for each experimental group/condition, given as a discrete number and unit of measurement |
| ☐ | ☒ | An indication of whether measurements were taken from distinct samples or whether the same sample was measured repeatedly |
| ☐ | ☒ | The statistical test(s) used AND whether they are one- or two-sided<br>*Only common tests should be described solely by name; describe more complex techniques in the Methods section.* |
| ☐ | ☒ | A description of all covariates tested |
| ☐ | ☒ | A description of any assumptions or corrections, such as tests of normality and adjustment for multiple comparisons |
| ☐ | ☒ | A full description of the statistics including central tendency (e.g. means) or other basic estimates (e.g. regression coefficient) AND variation (e.g. standard deviation) or associated estimates of uncertainty (e.g. confidence intervals) |
| ☐ | ☒ | For null hypothesis testing, the test statistic (e.g. *F*, *t*, *r*) with confidence intervals, effect sizes, degrees of freedom and *P* value noted<br>*Give P values as exact values whenever suitable.* |
| ☒ | ☐ | For Bayesian analysis, information on the choice of priors and Markov chain Monte Carlo settings |
| ☒ | ☐ | For hierarchical and complex designs, identification of the appropriate level for tests and full reporting of outcomes |
| ☒ | ☐ | Estimates of effect sizes (e.g. Cohen's *d*, Pearson's *r*), indicating how they were calculated |
| ☐ | ☒ | Clearly defined error bars<br>*State explicitly what error bars represent (e.g. SD, SE, CI)* |

*Our web collection on statistics for biologists may be useful.*

## Software and code

Policy information about availability of computer code

| | |
|---|---|
| Data collection | Software used for data collection includes the commercially available Nikon NIS Elements imaging software |
| Data analysis | Software used for data analysis includes the commercially available Nikon NIS Elements analysis software and the open source image analysis software ImageJ and MicrobeJ |

For manuscripts utilizing custom algorithms or software that are central to the research but not yet described in published literature, software must be made available to editors/reviewers upon request. We strongly encourage code deposition in a community repository (e.g. GitHub). See the Nature Research guidelines for submitting code & software for further information.

## Data

Policy information about availability of data

All manuscripts must include a data availability statement. This statement should provide the following information, where applicable:

- Accession codes, unique identifiers, or web links for publicly available datasets
- A list of figures that have associated raw data
- A description of any restrictions on data availability

The data that support the findings of this study are available from the corresponding author upon request

# Field-specific reporting

Please select the best fit for your research. If you are not sure, read the appropriate sections before making your selection.

☒ Life sciences ☐ Behavioural & social sciences ☐ Ecological, evolutionary & environmental sciences

For a reference copy of the document with all sections, see nature.com/authors/policies/ReportingSummary-flat.pdf

# Life sciences study design

All studies must disclose on these points even when the disclosure is negative.

| | |
|---|---|
| Sample size | Sample sizes were chosen based on historical data and no statistical methods were used to predetermine sample size. |
| Data exclusions | No data were excluded. However, in some instances, cells not meeting defined parameters, which would confound the analysis, were excluded. For Fig. 3b, cells that had already formed ComEA-mCherry foci at the start of imaging were excluded from the analysis. For pilus length measurements, pili that were already retracting when imaging began were excluded from the analysis. For extension and retraction rate calculations, only cells that made a single pilus that began extension and fully retracted within the 1 min window were analyzed. For microfluidic experiments using sheared pili, only DNA molecules that exhibited colocalization with pili during flow directional changes were analyzed, allowing for exclusion of glass-bound DNA from the analysis. Pili shorter than 0.5 µm were excluded from the microfluidic experiment analysis since their movement could not be resolved with directional flow changes. |
| Replication | All data are from a minimum of two independent experiments. All replication attempts were successful. |
| Randomization | There was no randomization in these experiments. Strains used were grown under similar conditions and were therefore equivalent at the start of experiments, and all differences observed are attributable to the genotype or treatment of the strains used under the testing conditions. |
| Blinding | No blinding was used in these experiments. Strains used were grown under similar conditions and were therefore equivalent at the start of experiments, and all differences observed are attributable to the genotype or treatment of the strains used under the testing conditions. |

# Reporting for specific materials, systems and methods

### Materials & experimental systems

| n/a | Involved in the study |
|---|---|
| ☐ | ☒ Unique biological materials |
| ☒ | ☐ Antibodies |
| ☒ | ☐ Eukaryotic cell lines |
| ☒ | ☐ Palaeontology |
| ☒ | ☐ Animals and other organisms |
| ☒ | ☐ Human research participants |

### Methods

| n/a | Involved in the study |
|---|---|
| ☒ | ☐ ChIP-seq |
| ☒ | ☐ Flow cytometry |
| ☒ | ☐ MRI-based neuroimaging |

## Unique biological materials

Policy information about availability of materials

| | |
|---|---|
| Obtaining unique materials | All bacterial mutant strains generated during this study are available from the corresponding author upon request. |